SEMARAK ILMU PUBLISHING

Semarak Journal of Thermal-Fluid Engineering

Journal homepage:
https://semarakilmu.my/index.php/sjotfe/index
ISSN: 3030-6639

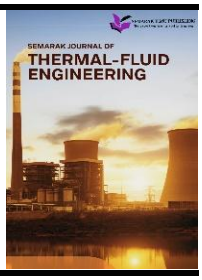

Analysis of Airflow over a Circular Cylinder at Various Reynolds Numbers

Ahmad Alif Ashraf Azwan[1*], Ahmad Danial Ahmad Junaidi[2], Ahmad Nadzim Jaafar[3], Aiman Akmal Mohd Farez[4], Eng Shao Tang[5]

[1] Faculty of Mechanical and Manufacturing Engineering, Universiti Tun Hussein Onn Malaysia, 86400 Parit Raja, Batu Pahat, Johor, Malaysia

ARTICLE INFO

Article history:
Received 12 January 2026
Received in revised form 8 February 2026
Accepted 6 March 2026
Available online 31 March 2026

Keywords:
Airflow; circular cylinder; Reynold number; boundary layer; flow separation;

ABSTRACT

This study presents a Computational Fluid Dynamics (CFD) analysis of airflow over a circular cylinder to investigate external flow behaviour with various Reynolds numbers. The investigation aims to analyse the effects of Reynolds number on velocity distribution, pressure distribution, and streamline patterns around the cylinder. A three-dimensional circular cylinder with a diameter of 20 mm was modelled and simulated using ANSYS Fluent. The governing equations of continuity and momentum were solved using the Finite Volume Method (FVM), with air at 25 °C as the working fluid. Uniform inlet velocities of 3 m/s, 6 m/s, and 9 m/s were applied, corresponding to Reynolds numbers of approximately 3360, 6720, and 10080. The flow field was analysed using velocity contours, pressure distribution, and streamline visualisations. The results showed that increasing Reynolds number within the subcritical turbulent wake regime led to earlier flow separation, larger wake regions, and stronger pressure gradients around the cylinder. High pressure was consistently observed at the stagnation point, followed by a low-pressure wake downstream. Overall, the study demonstrates that CFD can effectively capture the fundamental characteristics of external flow over a circular cylinder and provides clear insight into Reynolds number effects on boundary layer development, flow separation, and wake formation.

1. Introduction

The study of external flows is a fundamental area of study in fluid mechanics and is widely used to analyse flow behaviour around bluff bodies with various shapes such as circular cylinders, spheres, flat plates, rectangular cylinder, air foil and simplified car models [1]-[6]. Accurate prediction of velocity distribution, pressure variation, flow separation, and wake formation is essential for analysing external flow phenomena and for validating numerical approaches used in Computational Fluid Dynamics (CFD). The behaviour of flow around a circular cylinder is strongly governed by the Reynolds number, which determines the nature of boundary layer development, the onset of separation, and wake characteristics downstream of the cylinder [7]-[10].

* *Corresponding author.*
E-mail address: dd220034@student.uthm.edu.my

https://doi.org/10.37934/sjotfe.8.1.19a

Computational Fluid Dynamics (CFD) has become a powerful tool for analysing external flows over bluff bodies, providing detailed insight into velocity fields, pressure gradients, and wake formation. CFD allows the numerical resolution of governing equations over a discretized computational domain, capturing complex flow phenomena such as boundary layer development, flow separation, and vortex shedding [11]-[14]. The accuracy of CFD results depends strongly on mesh quality, turbulence modelling, and appropriate boundary condition selection. Previous studies have highlighted that mesh refinement is crucial for capturing the result accurately [15]-[17]. Mesh refinement near the cylinder surface and the wake region is critical for capturing flow separation and vortex dynamics accurately.

To address these challenges, the present study investigates airflow over a circular cylinder at various Reynolds numbers using CFD. The simulations focus on examining velocity contours, pressure distribution and streamline pattern to characterise the flow behaviour around the cylinder. This study aims to develop a clear understanding of external flow behaviour over circular cylinders and to demonstrate the capability of CFD in analysing fundamental external flow phenomena.

2. Methodology

2.1 Geometry of Computational Domain with Circular Cylinder

The computational domain for this study was designed to model external airflow over a three-dimensional circular cylinder as shown in Figure 1. The cylinder has a diameter of 20 mm and is positioned at the centre of the flow domain to minimize boundary interference. The total domain length was set to 300 mm, providing a sufficient downstream region for wake development. The distance from the inlet to the cylinder centre was maintained at 100 mm to ensure a uniform velocity profile before the flow interacts with the cylinder. The domain height was set to 200 mm to prevent confinement effects from the upper and lower boundaries, and the spanwise extrusion was set to 200 mm to account for the three-dimensional characteristics of the flow. This configuration provides an adequate balance between computational efficiency and physical accuracy, ensuring that the domain boundaries do not influence the flow field around the cylinder or the wake formation downstream.

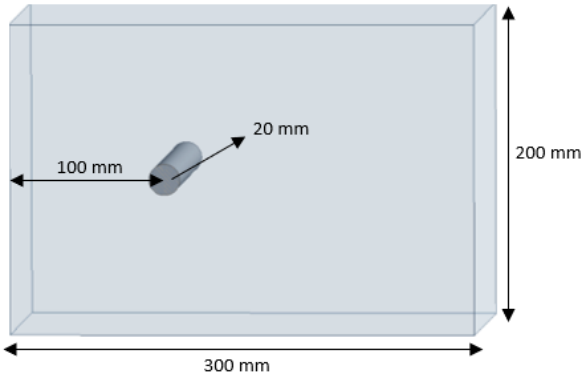

Fig. 1. Computational domain layout with circular cylinder

2.2 Discretization

In this study, the circular cylinder domain was discretized to enable numerical solution of the governing airflow equations. The continuous flow field around the cylinder was divided into finite

control volumes using a structured mesh to ensure sufficient resolution in both the near-wall and wake regions. This meshing approach allows accurate capture of boundary-layer development, flow separation, and wake formation behind the cylinder while maintaining a balance between computational efficiency and solution accuracy.

2.2.1 Mesh generation of the circular pipe

The computational domain around the circular cylinder was discretized using a multizone meshing approach to accurately represent the geometry and maintain flexibility in the mesh structure. Element size controls were applied throughout the domain to ensure a consistent mesh distribution, allowing for a balance between solution accuracy and computational efficiency. As shown in Figure 2, the multizone method provides uniform element sizing around the cylinder and in the surrounding flow field. Mesh quality metrics such as skewness and orthogonality were monitored to ensure numerical stability and reliability of the simulation results.

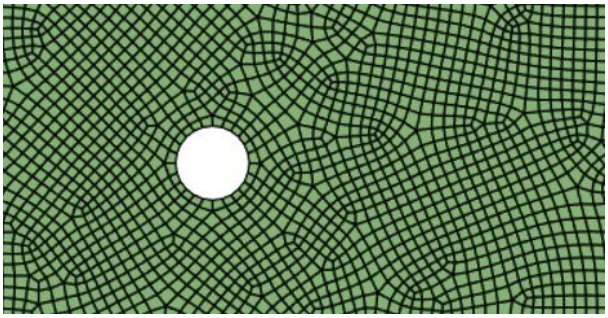

Fig. 2. Computational mesh for fluid domain

2.2.2 Grid independence test

The Grid Independence Test (GIT) is a crucial step in Computational Fluid Dynamics (CFD) analysis used to ensure that the numerical results are not dependent on the mesh size or grid resolution. In the grid independence process, several mesh sizes are tested by running simulations under the same boundary conditions and physical parameters. When further refinement of the mesh produces negligible changes in these parameters, the solution is considered grid independent. This procedure helps balance accuracy and computational efficiency by selecting a mesh that provides reliable results without unnecessary computational cost [18]-[20].

2.3 Governing Equation

The airflow around the circular cylinder was modelled as steady, incompressible, and Newtonian external flow, governed by the continuity and Navier–Stokes equations. The continuity equation ensures mass conservation and is expressed as:

$$\nabla \cdot V = 0 \tag{1}$$

while the momentum equation for incompressible flow is given by:

$$\rho(V \cdot \nabla)V = -\nabla p + \mu \nabla^2 V \tag{2}$$

where V is the velocity vector, p is the static pressure, ρ is the air density and μ is the dynamic viscosity of air.

The Reynolds number for the external flow over the circular cylinder is defined as:

$$Re = \frac{\rho UD}{\mu} \tag{3}$$

where U is the inlet velocity and D is the cylinder diameter. For inlet velocities of 3 m/s, 6 m/s, and 9 m/s, the corresponding Reynolds numbers are approximately 3360, 6720, and 10080 respectively. The k–ω Shear Stress Transport (SST) turbulence model was employed for higher Reynolds number cases. The turbulent eddy viscosity is calculated as:

$$\mu_t = \frac{\rho a_1 k}{max\,(a_1\omega, SF_2)} \tag{4}$$

where k is the turbulence kinetic energy, ω is the specific dissipation rate, S is the magnitude of the strain rate, F_2 is the blending function and a_1 is a model constant.

2.4 Boundary Condition

A uniform velocity inlet condition was applied at the upstream boundary with inlet velocities of 3 m/s, 6 m/s, and 9 m/s corresponding to increasing Reynolds numbers. The downstream boundary was defined as a pressure outlet with a gauge pressure of 0 Pa. The top and bottom boundaries of the computational domain were assigned as symmetry planes to eliminate wall friction effects and maintain a free-stream environment. The cylinder surface was treated as a no-slip wall, enforcing zero velocity at the solid–fluid interface. Air at 25 °C was used as the working fluid, with a density of 1.225 kg/m³ and a dynamic viscosity of 1.789×10^{-5} Pa·s representing standard atmospheric conditions. All simulations were performed under steady-state conditions using the k–ω SST turbulence model for all velocity cases to effectively capture boundary-layer behaviour, flow separation, and wake formation behind the circular cylinder.

2.5 Analysis

2.5.1 Velocity analysis

Velocity is a key parameter in understanding airflow behaviour around a circular cylinder. Velocity reflects how the flow develops and separates at different Reynolds numbers. Extracting the velocity distribution around the cylinder allows for identification of flow acceleration, deceleration, and wake formation. Analysing the velocity profiles around the cylinder surface and in wake region provides insight into the balance between viscous and inertial forces. This analysis also highlights critical regions such as the stagnation point, boundary layer development, and maximum velocity regions which are essential for understanding aerodynamic forces on the cylinder.

2.5.2 Pressure analysis

Pressure distribution around a circular cylinder is crucial for characterising aerodynamic loading and identifying flow separation points. Extracting the pressure along the cylinder surface allows evaluation of the pressure gradient, which directly influences drag and wake formation. At low

Reynolds numbers, the pressure drops along the cylinder are smooth and symmetric, while at higher Reynolds numbers, adverse pressure gradients lead to earlier flow separation and vortex shedding. By analysing the pressure alongside velocity, the study assesses the flow regime and validates the CFD ability to capture flow behaviours at different Reynolds numbers. This provides a comprehensive understanding of the interaction between pressure forces and flow patterns around bluff bodies.

2.5.3 Streamline analysis

Streamlines provide a visual representation of flow patterns around the cylinder. It shows the direction and curvature of airflow at various Reynolds numbers. At low Reynolds numbers, streamlines remain smooth and closely follow the cylinder contour. As the Reynolds number increases, streamlines begin to separate from the cylinder surface forming recirculation zones and vortex shedding in the wake region. Analysing streamlines complements velocity and pressure data by clearly illustrating flow attachment, separation, and wake dynamics. This provides an intuitive understanding of the airflow behaviour on the cylinder.

3. Results

3.1 Grid Independence Test Result

The grid independence test was conducted to ensure that the numerical results are not significantly influenced by mesh resolution. Figure 3 presents the velocity distribution along the axial distance for three different mesh configurations. It can be observed that all three meshes predict a similar velocity trend along the flow direction. However, Mesh 1 shows a noticeable deviation near the developing flow region. In contrast, the velocity profiles for Mesh 2 and Mesh 3 overlap closely suggesting that further mesh refinement produces negligible changes in the predicted velocity field. Based on these observations, Mesh 3 was selected for subsequent simulations as it provides better accuracy.

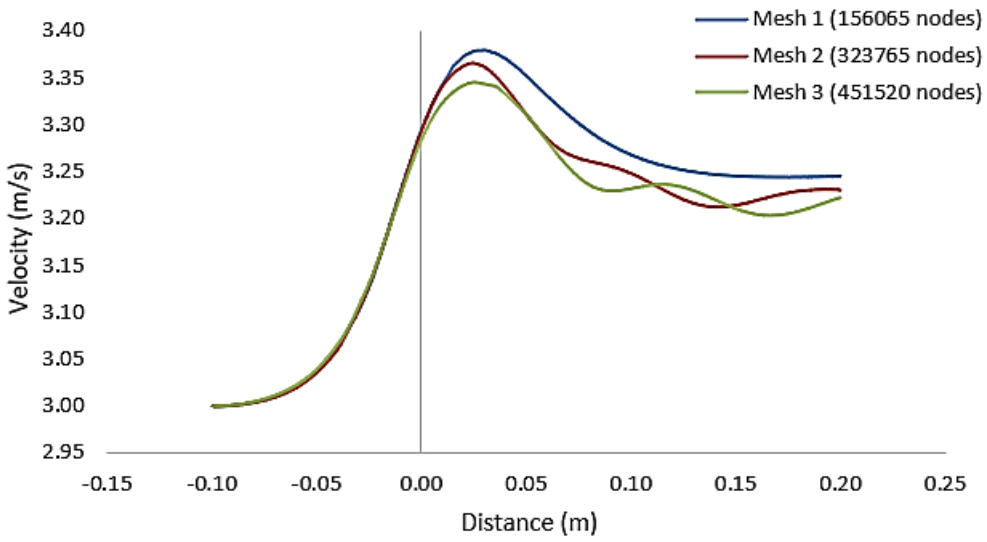

Fig. 3. Velocity chart for grid independence test

Velocity was chosen as the key parameter for the grid independence test because it effectively represents the development of the external flow field and is highly sensitive to mesh quality in regions of flow separation, and wake formation around the circular cylinder. Since the difference in

velocity distribution between Mesh 2 and Mesh 3 is minimal, the results confirm that the solution has reached mesh independence and can be confidently used for further analysis and comparison with theoretical predictions.

3.2 Velocity Contour of Three Different Reynolds Numbers

The velocity contours illustrate the effect of increasing inlet velocity on the flow behaviour around the circular cylinder. Figure 4 shows the velocity magnitude contours around the circular cylinder for three different inlet velocities of 3 m/s, 6 m/s, and 9 m/s. These cases correspond to increasing Reynolds numbers and are used to examine the influence of flow velocity on boundary layer development, flow separation and wake formation. By comparing the velocity fields at different inlet conditions, the flow structure and wake behaviour behind the cylinder can be clearly observed.

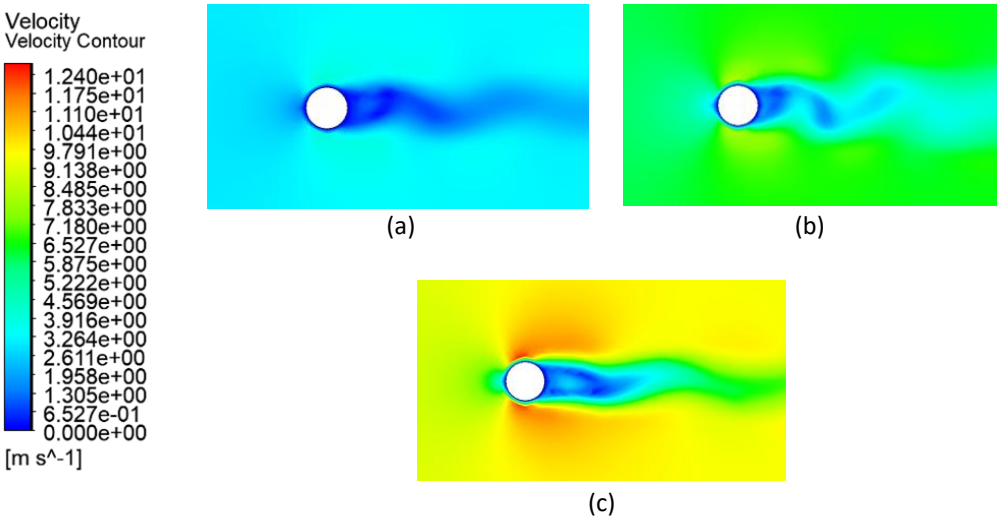

Fig. 4. Velocity contour of inlet velocities (a) 3 m/s (b) 6 m/s (c) 9 m/s

The flow remains largely laminar at velocity 3m/s and attached along the cylinder surface. The formation of a small and steady wake region at the rear indicates dominant viscous effects and minimal flow separation. As the velocity increases to 6 m/s, the flow begins to separate earlier from the cylinder surface. The wake region becomes wider, indicating the onset of unsteady flow characteristics. At the highest velocity of 9 m/s, the flow transitions into a turbulent forming a distinct von Kármán vortex street. This pattern demonstrates that as the Reynolds number increases, inertial forces become more dominant, causing larger flow separation and an elongated wake region downstream of the cylinder.

3.3 Pressure Contour of Three Different Reynold Numbers

The results obtained from the CFD simulation as shown in Figure 5 illustrate the variation of pressure distribution around the circular cylinder at different inlet velocities. For all cases, a high-pressure region is observed at the front stagnation point of the cylinder, followed by a pressure reduction along the surface due to flow acceleration and separation. This pressure behaviour is characteristic of external flow over a bluff body and becomes increasingly pronounced as the inlet velocity increases.

The pressure contours for the inlet velocity of 3 m/s remain nearly symmetric about the cylinder. The pressure recovery at the rear of the cylinder is limited, indicating a small and steady wake region

with minimal flow separation. When the inlet velocity is increased to 6 m/s, a larger pressure difference develops between the front and rear surfaces of the cylinder. The low-pressure region downstream expands as flow separation becomes more significant. At the highest inlet velocity of 9 m/s, the pressure gradient around the cylinder becomes highly pronounced. The stagnation pressure at the front remains high, while a strong low-pressure wake forms downstream of the cylinder. This indicates flow separation and vortex shedding in the wake region. Overall, the pressure contours clearly demonstrate that increasing the Reynolds number intensifies the pressure difference across the cylinder.

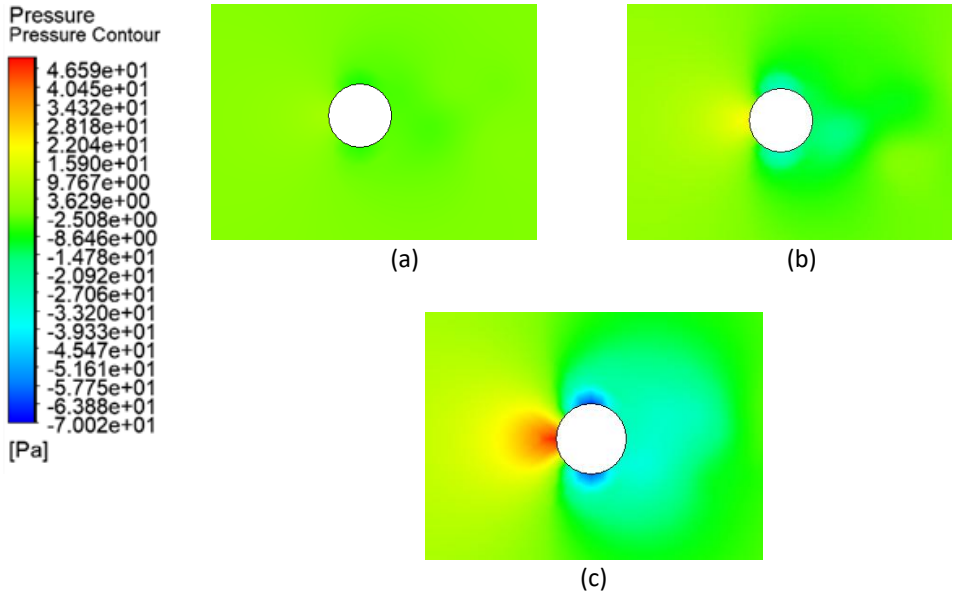

Fig. 5. Pressure contour of inlet velocities (a) 3 m/s (b) 6 m/s (c) 9 m/s

3.4 Velocity Streamline of Three Different Reynold Numbers

The streamline patterns obtained from the CFD simulation as shown in Figure 6 illustrate the effect of increasing inlet velocity on the flow structure around the circular cylinder. For all cases, the streamlines follow the cylinder surface before separating downstream forming a wake region characteristic of external flow over a bluff body. As the inlet velocity increases, the extent of flow separation and wake development becomes more pronounced. At an inlet velocity of 3 m/s, the streamlines remain smooth and closely following the cylinder surface with only slight separation occurring downstream.

When the inlet velocity is increased to 6 m/s, the streamlines exhibit greater curvature around the cylinder and flow separation occurs earlier along the surface. This leads to the formation of a wider and longer wake region downstream of the cylinder. At the highest inlet velocity of 9 m/s, the streamline patterns show significant distortion in the wake region with alternating flow paths forming downstream of the cylinder. The wake becomes larger and more complex, indicating strong flow separation and unsteady wake development. Overall, the streamline results demonstrate that increasing the Reynolds number intensifies flow separation and wake formation, leading to more complex and unstable flow behaviour around the circular cylinder.

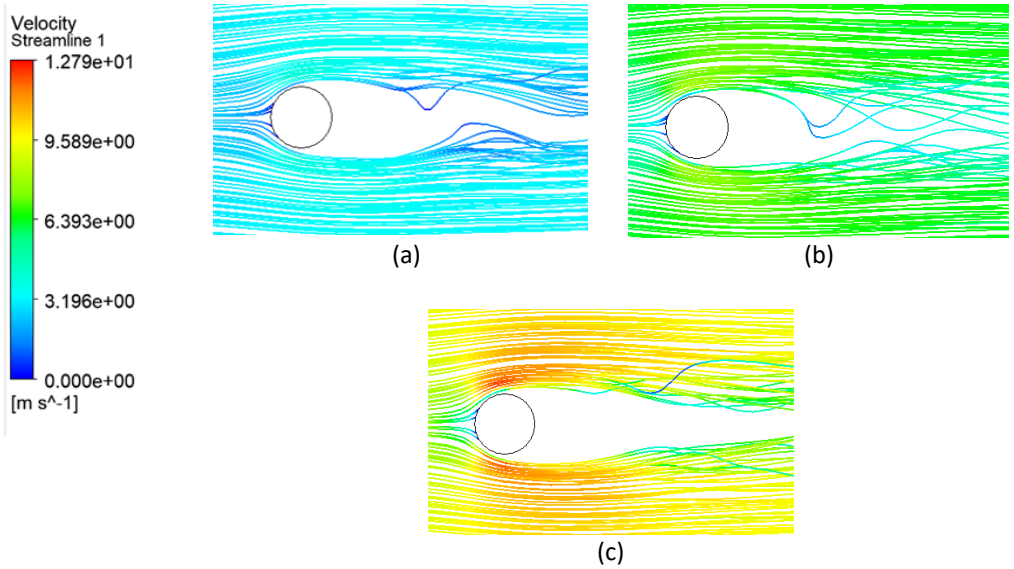

Fig. 6. Velocity streamline of inlet velocities (a) 3 m/s (b) 6 m/s (c) 9 m/s

4. Conclusions

In conclusion, the CFD analysis successfully achieved the objective of investigating airflow behaviour over a circular cylinder at Reynolds numbers ranging from approximately 3,360 to 10,080, corresponding to inlet velocities of 3 m/s, 6 m/s, and 9 m/s. The velocity contours demonstrated that increasing the Reynolds number resulted in earlier flow separation and a progressively larger wake region downstream of the cylinder. Pressure distributions consistently showed a high stagnation pressure at the front of the cylinder and an increasing pressure difference between the front and rear surfaces. Streamline patterns further confirmed the transition from attached flow at lower Reynolds numbers to more separated and unstable wake flow at higher Reynolds numbers. Overall, the results demonstrate that the CFD model can capture the fundamental characteristics of external flow over a circular cylinder and successfully meet the objective of analysing Reynolds number effects on velocity, pressure, and streamline pattern.

References

[1] Hishikar, Prafull, S. K. Dhiman, Anil Kumar Tiwari, and Vivek Kumar Gaba. "Analysis of flow characteristics of two circular cylinders in cross-flow with varying Reynolds number: a review." *Journal of Thermal Analysis and Calorimetry* 147, no. 10 (2022): 5549-5574. https://doi.org/10.1007/s10973-021-10933-w

[2] Li, Junwei, and Benmou Zhou. "The symmetry and stability of the flow separation around a sphere at low and moderate Reynolds numbers." *Symmetry* 13, no. 12 (2021): 2286. https://doi.org/10.3390/sym13122286

[3] El Khatib, Atef, Ahmad Al Miaari, Hassan Assoum, Ahmad Salem, and Ali Hammoud. "A Review on Flow Regimes and Aeroacoustic Coupling in Subsonic Flow Around Flat Plates." *Arabian Journal for Science and Engineering* (2025): 1-25. https://doi.org/10.1007/s13369-024-09937-z

[4] Tahir, Neelam, Noor Zeb Khan, Waqas Sarwar Abbasi, Muhammad Ayaz, Zahoor Ahmad, and Tareq Alhmiedat. "Numerical investigation of wake dynamics and flow interference effects on fluid-structure interaction of dual side-by-side rectangular cylinders: A Lattice Boltzmann study." *Results in Engineering* (2025): 107578. https://doi.org/10.1016/j.rineng.2025.107578

[5] Mustak, Rubiat, and Mohammad Mashud. "Recent advances in flow separation control of airfoils through surface grooves." *AIP Advances* 15, no. 11 (2025). https://doi.org/10.1063/5.0290804

[6] Mariaprakasam, Rafiqi Daniel Ramadhan, Shabudin Mat, P. Mohd Samin, Norazila Othman, Mastura Ab Wahid, and Mazuriah Said. "Review on flow controls for vehicles aerodynamic drag reduction." *Journal of Advanced Research in Fluid Mechanics and Thermal Sciences* 101, no. 1 (2023): 11-36. https://doi.org/10.37934/arfmts.101.1.1136

[7] Ali, Mariyam, and Abdur Rahim. "Numerical investigation of vortex shedding: a comparative analysis of pair of cylinder with different configurations." *Sādhanā* 50, no. 3 (2025): 217. https://doi.org/10.1007/s12046-025-02898-5

[8] Krishna Chaitanya, N. V. V., and Dipankar Chatterjee. "Mixed convective flow past counter-rotating side-by-side cylinders at low Reynolds number." *Numerical Heat Transfer, Part A: Applications* 83, no. 2 (2023): 141-159. https://doi.org/10.1080/10407782.2022.2084300

[9] Alfredsson, P. Henrik, Kentaro Kato, and R. J. Lingwood. "Flows over rotating disks and cones." *Annual Review of Fluid Mechanics* 56, no. 1 (2024): 45-68. https://doi.org/10.1146/annurev-fluid-121021-043651

[10] Huera-Huarte, Francisco. "Vortex-induced vibration of flexible cylinders in cross-flow." *Annual Review of Fluid Mechanics* 57 (2025): 285-310. https://doi.org/10.1146/annurev-fluid-022724-014235

[11] Wahyuni, F., Harinaldi, Nasruddin, and J. Julian. "Surface modifications for drag reduction in flow around circular cylinders: a critical review." *Journal of Engineering and Applied Science* 72, no. 1 (2025): 237. https://doi.org/10.1186/s44147-025-00795-6

[12] Chashechkin, Yuli D. "Discrete and continuous symmetries of stratified flows past a sphere." *Symmetry* 14, no. 6 (2022): 1278. https://doi.org/10.3390/sym14061278

[13] Abbas, Zaheer, Mohtashim Mansoor, Muzaffar Habib, and Zahid Mehmood. "MEMS sensors for flow separation detection." *Microsystem Technologies* 29, no. 9 (2023): 1253-1280. https://doi.org/10.1007/s00542-023-05513-x

[14] Manoj Dundi, T., K. Sridhar, S. Vidhi, T. Sai Krishna, and O. Shailu. "CFD analysis of external flow vortex shedding in flow over a ribbed and grooved cylinder." In *International Conference on Mechanical Engineering: Researches and Evolutionary Challenges*, pp. 595-609. Singapore: Springer Nature Singapore, 2023. https://doi.org/10.1007/978-981-97-0918-2_48

[15] Zhu, Yongzheng, Shiji Zhao, Yuanye Zhou, Hong Liang, and Xin Bian. "An unstructured adaptive mesh refinement for steady flows based on physics-informed neural networks." *Journal of Computational Physics* (2025): 114283. https://doi.org/10.1016/j.jcp.2025.114283

[16] Perera, Roberto, and Vinamra Agrawal. "Multiscale graph neural networks with adaptive mesh refinement for accelerating mesh-based simulations." *Computer Methods in Applied Mechanics and Engineering* 429 (2024): 117152. https://doi.org/10.1016/j.cma.2024.117152

[17] Li, Yezhan, and Tsubasa Okaze. "Application of polyhedral meshes in large-eddy simulation of building array flow fields within neutral and unstable boundary layers." *Building and Environment* 263 (2024): 111846. https://doi.org/10.1016/j.buildenv.2024.111846

[18] Liu, Huan, Farhad Hussain, Chew Lim Tan, and Manoranjan Dash. "Discretization: An enabling technique." *Data Mining and Knowledge Discovery* 6, no. 4 (2002): 393-423. https://doi.org/10.1023/A:1016304305535

[19] Zulkifli, Zulaika, NH Abdul Halim, Z. H. Solihin, J. Saedon, A. A. Ahmad, A. H. Abdullah, N. Abdul Raof, and M. Abdul Hadi. "The analysis of grid independence study in continuous disperse of MQL delivery system." *Journal of Mechanical Engineering and Sciences* (2023): 9586-9596. https://doi.org/10.15282/jmes.17.3.2023.5.0759

[20] Almohammadi, K. M., D. B. Ingham, L. Ma, and M. Pourkashan. "Computational fluid dynamics (CFD) mesh independency techniques for a straight blade vertical axis wind turbine." *Energy* 58 (2013): 483-493. https://doi.org/10.1016/j.energy.2013.06.012